(To Appear) *Experiments in Fluids* – D. P. Hart
Similar to paper in , 9th International Symposium on Applications of Laser Techniques to Fluid Mechanics, July 13-16, 1998, Lisbon, Portugal.

PIV Error Correction

Douglas P. Hart

Department of Mechanical Engineering, Massachusetts Institute of Technology, Cambridge, MA 02139-4307, USA

Abstract. *A non-post-interrogation method of reducing subpixel errors and eliminating spurious vectors from particle image velocimetry (PIV) results is presented. Unlike methods that rely on the accuracy or similarity of neighboring vectors, errors are eliminated before correlation information is discarded using available spatial and/or temporal data. Anomalies are removed from the data set through direct element-by-element comparison of the correlation tables calculated from adjacent regions. The result is a correction method that improves subpixel accuracy and effective spatial resolution and is highly robust to out-of-boundary particle motion, particle overlap, inter-particle correlations, and electronic and optical imaging noise.*

Keywords. PIV, correlation, error correction, super-resolution, recursive-correlation

1 Introduction

Because Particle Image Velocimetry (PIV) is based on the statistical correlation of imaged subregions to determine local flow velocities, it is subject to inherent errors that arise from finite tracer particle numbers, sample volume size, and image resolution. These errors, in extreme cases, are relatively easy to detect as they tend to vary substantially from neighboring vectors in both magnitude and direction. Despite this, correcting these errors is often difficult as present computer algorithms lack the innate pattern recognition ability of humans. Furthermore, such errors need not present themselves in obvious manners. Velocity vectors determined by correlating finite subregions of tracer particle images are often biased to varying degrees by; out-of-boundary particle motion, correlations occurring between unmatched particle pairs, particle overlap, non-uniform particle distribution, and variations in image intensity [Keane et. al. 1992; Prasad et. al. 1992; Westerweel et. al. 1993, 1994, 1997; Raffel et. al. 1994; Lourenco et. al. 1995; Fincham et. al. 1997]. Such errors along with errors associated with excessive velocity gradients and the finite sample volume size necessary to image a statistically meaningful number of tracer particles, limit accuracy and resolution and thus, limit the usefulness of PIV.

Currently, the most widely used and accepted technique to eliminate correlation errors is to compare vectors with their neighbors to determine if they are in some statistical or physical sense inconsistent. This technique, analyzed in detail by Westerweel (1994), is based on the assumption that vectors resulting from correlation errors are far removed in magnitude and/or direction from neighboring vectors. It assumes that the resolution of PIV data is high enough and the flow features benign enough that apparent discontinuities in the flow will not present themselves and be eliminated. It is a method of detecting errors and not a method of resolving tracer particle displacement. Detailed correlation information is discarded before interrogation. Consequently, errors can only be eliminated from the results and replaced by interpolated values. Furthermore, this error correction method addresses only the most obvious of correlation errors and does not address the more subtle problems that severely limit subpixel accuracy and resolution. Although extremely useful, post-interrogation error correction is not ideal.

Presented herein is a robust and computationally efficient method of removing errors from PIV results and resolving vectors from regions where noise in the correlation table obscures tracer particle displacement. This method, based on an element-by-element comparison of the correlation tables taken from adjacent regions, does not rely on the accuracy or similarity of neighboring vectors, as does post-interrogation correction. Errors are directly eliminated from the correlation data improving spatial resolution and subpixel accuracy.

2 Correlation Errors

PIV images are typically processed by subdivision into a regular grid of overlapping windows that bound regions of similar flow velocity; a velocity vector is then found for each window by autocorrelation or cross-correlation. Autocorrelation and cross-correlation produces a table of correlation values over a range of displacements, and the overall displacement of particles in the window is represented by a peak in this correlation table. Errors occur primarily from insufficient data whether from a lack of imaged flow tracers or poor image quality, and/or from correlation anomalies generally resulting from unmatched tracer images within the correlated sample volume. Currently, errors are held to a minimum by using high resolution imaging equipment and carefully controlling seeding density and interrogation size.

Seeding Density

As the number of tracer particles within a sample volume increases, the probability of any finite region existing with a particle set of similar intensity and pattern decreases. Thus, the probability of obtaining an accurate measure of the displacement of a set of particles using correlation increases as the number of particles increases. Keane and Adrian (1992) demonstrated this by showing that the number of spurious vectors that appear in PIV data drop dramatically as particle numbers within correlated subregions are increased to an average of about ten particle images per region. Very high seeding densities, however, can alter the characteristics of the flow being measured and make it difficult if not impossible to adequately illuminate and image tracer particles within a specific region of interest. Consequently, there generally exists a limit to the density that a flow can be seeded.

Interrogation Size

An alternative is to increase the size of the sample volume. This increases the number of tracer particles in the interrogation region without increasing the seeding density. Furthermore, it reduces correlation anomalies associated with particles entering and exiting the sample volume in the time between exposures. As the sample volume is increased, a smaller fraction of particles enter and exit relative to the total number of particles that remain within the sample volume between exposures. Consequently, there is a reduction in correlation values from unmatched particle images between exposures. Keane and Adrian (1992) conjectured and Westerweel, Dabiri and Gharib (1997) demonstrated that significant errors due to an asymmetry in the peak correlation within the correlation table are associated with this phenomenon. Westerweel *et. al.* (1997) went on to show that these *bias errors* could be significantly reduced by correlating with an interrogation window offset by the integer value of local particle pixel displacement. This effectively eliminates out-of-boundary particle motion and the correlation anomalies associated with them. There is a significant reduction in error as long as the local particle displacement is approximately an integer value. It is less effective when the residual of the local displacement is around a half-pixel. Unfortunately, this technique addresses only errors due to translational flow within the interrogation plane and does not account for asymmetries in the correlation table caused by other sources such as out-of-plane particle motion or velocity gradients.

In particular, large velocity gradients are troublesome, not only because it introduces bias errors, but also because it limits the maximum interrogation size. A large local velocity gradient can result in unequal particle displacements causing one part of an interrogation region to correlate at a significantly different location than another part. The correlation table, rather than having one prominent peak representing the average particle displacement in a region, has multiple peaks or one shorter wider peak representing individual particle correlations from different areas in the sample volume. Increasing the sample volume exacerbates the problem as the relative separation in individual particle correlations from one region to another due to gradients in the flow increases as well. Consequently, there is an upper limit to both the seeding density and the interrogation size used to process PIV data. These limits severely constrain the use of PIV and force an often-unsatisfactory compromise between processing accuracy, resolution, and robustness.

3 Correlation Error Correction

Both errors resulting from insufficient data and errors caused by correlation anomalies can be eliminated during processing, regardless of the method of correlation, simply by multiplying the correlation table generated during processing by the correlation table generated from one or more adjacent regions.

This *correlation error correction* technique is illustrated in Fig.1. Here, the correlation table calculated during processing of one region (Fig. 1*A*) is multiplied, element-by-element, by the correlation table calculated from an adjacent region that overlaps the first region by fifty-percent (Fig. 1*B*). Neither of the correlation tables in this example (Fig. 1*A* or 1*B*) has a discernable peak representing tracer particle displacement. The resulting correlation table (Fig. 1*C*), however, has very few correlation anomalies and has a very prominent correlation peak in the lower right hand corner.

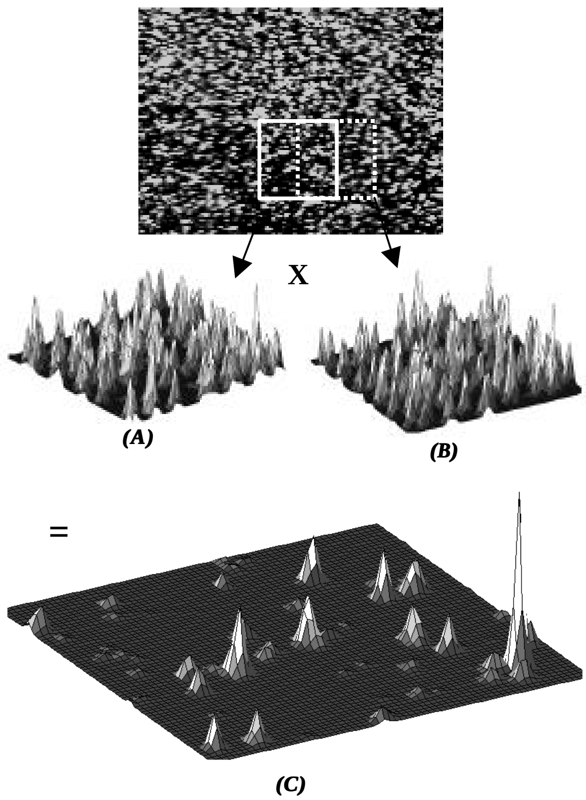

Figure 1. *– Elimination of correlation anomalies by multiplying the correlation tables from adjacent regions. Correlation values that do not appear in both tables are eliminated allowing tracer particle displacement to be resolved.*

Correlation error correction is effectively a correlation of two or more correlation tables. It is not an averaging technique. Any correlation value that does not appear in each of the combined correlation tables is eliminated from the resulting table. As the probability of exactly the same anomalies appearing in different regions is very small, correlation anomalies, regardless of their source, are eliminated from the data. Conversely, correlation values that are identical in location and magnitude in each of the combined tables are amplified. Thus, even if tracer particles displacement is not discernable in any of the combined correlation tables, multiplied together, the peak is either easily resolved or it becomes evident that at least one of the combined tables does not contain sufficient information to resolve particle displacement.

Consider the two non-overlapping NxN adjacent interrogation regions shown in Figure 2*A*. If the velocity within these interrogation regions is linear such that $\vec{V} = \left(v_x \cdot \frac{x}{N} + v_o \right)\hat{j}$ then the peaks resulting from the correlation of these regions fall within the ***y***-displacement envelope defined by

$$f_y = \int_{-N/2}^{N/2} e^{-\left(\frac{y - v_x \cdot \frac{x}{N} - v_o}{r}\right)^2} dx$$

where r is the characteristic tracer particle radius. This envelope, graphed in Fig. 2*B* and 2*C*, has a Gaussian profile that is elongated in the direction of the velocity gradient and centered on the average velocity within the interrogation region. If the correlation tables from the two regions are multiplied element-by-element together, the resulting correlation peak is forced into the axisymmetric Gaussian profile shown in Fig. 2*D*. The symmetry of this envelope allows accurate subpixel interpolation. Furthermore, correlation errors from non-uniform illumination and from non-uniform tracer particle distribution within the interrogation regions that result in asymmetric correlation profiles are minimized as they have little influence on the combined profile, Fig. 3. This forced symmetry can be accomplished in the ***y***-direction as well simply by combining correlation tables from more than two adjacent interrogation regions located along both the ***x*** and ***y*** directions.

Correlation error correction is not equivalent to correlating a larger region equal to the sum of the combined regions. Such a correlation would not eliminate correlation anomalies. It would, assuming no local velocity gradient, only strengthen the correlation peak representing the average particle displacement in the combined regions. This is not true of correlation error correction. The correlation peak found in the table resulting from correlation error correction is weighted to the displacement of the tracer particles within the overlap of the combined regions. Information within the overlapping regions identically effect the values in all of the correlation tables equally and are, therefore, not removed during processing. Particle displacements in regions outside the overlap influence the calculated displacement but to an extent that depends on the similarity in displacement. Thus, rather than a reduction in resolution, there is an improvement that depends on the size of the overlap and the gradient of the velocity relative to the size of the sample volume.

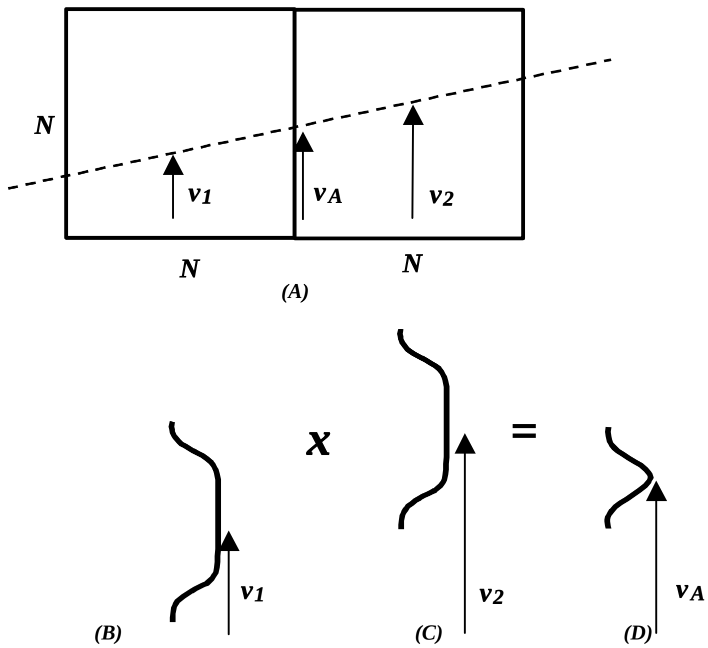

Figure 2. *– Forced correlation symmetry by multiplying the correlation tables from adjacent regions. Correlation values that fall outside one particle radius are eliminated forcing the correlation profile into a near axisymmetric shape centered on the tracer particle displacement of the adjoining region. The symmetry of this correlation profile aids in estimating subpixel displacement.*

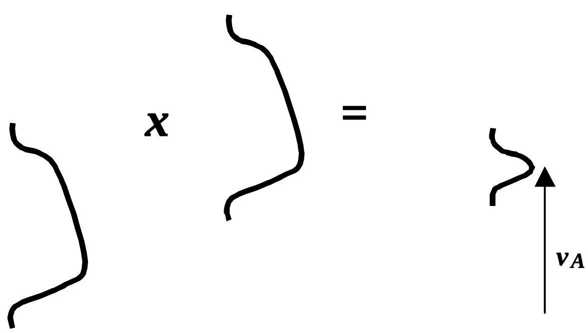

Figure 3. *– Correction of asymmetry in correlation profiles occurring due to non-uniform illumination and non-uniform seeding within interrogation regions. Because correlation error correction forces the correlation peak into a symmetric profile, velocity and illumination gradient errors that occur from correlating finite subregions are minimized.*

The level of effectiveness of this error correction technique at reducing correlation anomalies increases as the size of the overlapped region decreases. This is due to a reduction in the level of shared information. Correlation anomalies from image data within the overlapped region, appear equally in the correlation tables of each of the combined regions and are thus, not removed when the tables are multiplied together. Hence, it is desirable to maintain as small an overlap between combined regions as possible. Valid correlations, however, can be eliminated from regions with high velocity gradients if the flow results in a relative particle displacement greater than about one particle diameter between the combined regions. This is illustrated in Fig. 4 where correlation tables from two non-overlapping regions are multiplied together element-by-element. The resulting table has a much reduced correlation peak compared to Fig.1. The peak, found in the lower right hand corner of this table, represents tracer particle displacements that are roughly one particle image diameter apart.

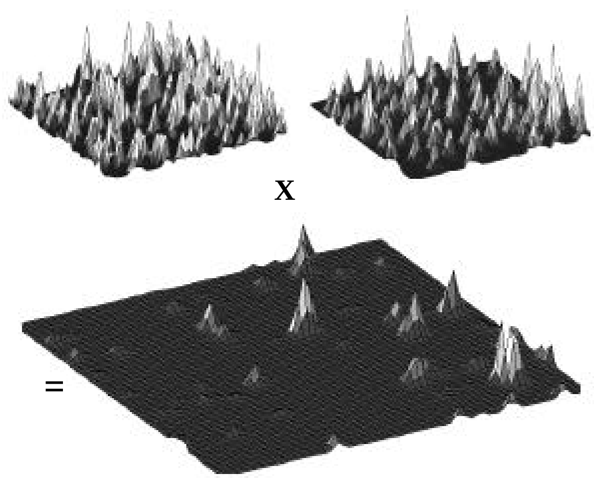

Figure 4. *– Illustration of the effect of an excessive particle displacement between regions using correlation error correction. Signal strength is significantly reduced when tables are multiplied from regions where particle displacement differs by more than one particle diameter.*

The optimum overlap between combined regions depends, largely, on the characteristics of the flow and the seeding density. In order to improve spatial resolution, most correlation algorithms currently use a fifty-percent overlap in adjacent regions [Willert et. al. 1991]. Therefore, fifty-percent overlapping regions were selected to evaluate the performance of this error correction method.

Although perhaps not optimum, this overlap serves as a baseline for comparison and it has been demonstrated to efficiently remove spurious vectors (Fig. 5).

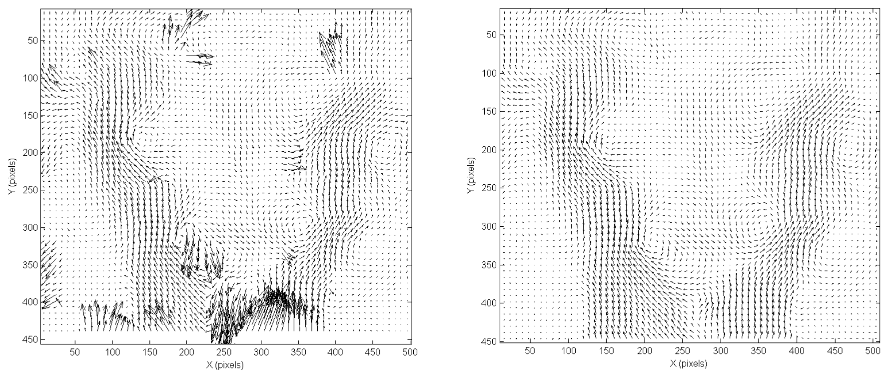

(A) ***(B)***

Figure 5. – *Elimination of processing errors using correlation error correction. 3(A) represents uncorrected PIV results of a high Reynolds number swirling flow undergoing sudden expansion. 3(B) illustrates the same data processed using correlation error correction. The corrected vectors are true tracer particle displacements and not interpolated values.*

4 Performance

Using Monte Carlo simulations, the effects of large velocity gradients, out-of-boundary motion, and seeding density on the performance of correlation error correction were investigated. Pairs of synthetic images were generated with randomly distributed 256-grayscale Gaussian particle images 4 pixels in diameter. Processing was done using FFT spectral correlation on 64*x*64 pixel interrogation regions with 10 particle images per region. Results using correlation error correction were compared with non-spurious results from uncorrected data. (For simplicity, spurious vectors are defined here as vectors that have a ***x*** or ***y*** component greater than 0.5 pixels from the imposed mean displacement within the interrogation region.)

Correlation Signal-to-Noise Ratio

By eliminating correlation anomalies, correlation error correction significantly enhances the correlation signal-to-noise ratio. This allows particle displacement to be resolved from regions that would otherwise be obscured by correlated noise from unmatched tracer particle images, inter-particle correlations, and electronic and optical imaging noise. To illustrate this, synthetic images representing 16 *pixel* translational displacement were created with the equivalent of 32 *pixel* out-of-plane motion (50% of the equivalent interrogation plane thickness). Using 64*x*64 *pixel* interrogation regions that overlapped 50%, 12% of the calculated vectors were determined to be spurious when processed *without* correlation error correction. When processed *with* correlation error correction, 70% of these spurious vectors were resolved and the remaining 30% were removed from the data set.

Fig. 6 illustrates the improved performance of correlation error correction. Here the correlation signal-to-noise ratio (SNR) is defined as the ratio between the second highest and highest correlation peaks. The percentage of the spurious and valid vectors with correlation signal strength (1-1/SNR) greater than indicated by the ***x*** axis are plotted for data processed with and without correlation error correction. When processed with correlation error correction, 90% of the valid vectors and none of the spurious vectors have a signal strength greater than 50%. In contrast, when the same data is processed without correlation error correction, only 30% of the valid vectors (shown as a dashed line) have a signal strength greater than 50%.

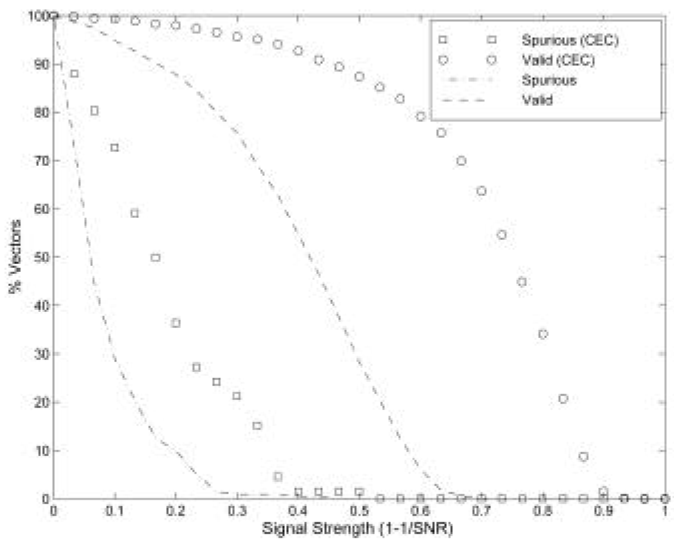

Figure 6. *– Improved signal-to-noise ratio resulting from correlation error correction (CEC). The percentage of spurious and valid vectors with correlation signal strengths greater than indicated by the x axis are compared for data processed with and without correlation error correction.*

Spurious Vector Elimination

The improved correlation signal-to-noise ratio resulting from correlation error correction, not only increases the number of valid vectors calculated, but also allows spurious vectors to be easily detected and removed. Two methods exist for detecting spurious vectors; (1) a threshold can be set and all vectors with a correlation signal-to-noise ratio less than the threshold discarded, or (2) the correlation peak resulting from the combined correlation tables can be compared with the peaks from each of the tables. If the peak in the combined table exists as a peak in at least one of the other tables, it is likely to represent tracer particle displacement.

The threshold method, although effective at removing spurious vectors, can result in the loss of significant numbers of valid vectors. In the previous example, illustrated by Fig. 6, if a threshold level of 50% is used for the correlation signal-to-noise ratio, all of the spurious vectors are removed but at a cost of about 10% of the valid vectors. This is not as excessive as it first appears considering that the valid vectors removed are the ones with the lowest correlation signal-to-noise ratio and are thus, the ones most likely to contribute to subpixel displacement inaccuracies in the results. Furthermore, correlation error correction in this example results in an 8% increase in the number of valid vectors calculated. Thus, a 10% loss in the number of valid vectors while eliminating spurious vectors results in only 2% fewer valid vectors than would be calculated without correlation error correction – a small price for improved accuracy.

Nonetheless, the second method of detection, peak comparison, provides a more robust and direct way of eliminating spurious vectors. This method of detection is similar to the *median* method suggested by Westerweel (1994) except that it is based on data that exists only in the interim of processing. The probability that the peak correlation value from a spurious vector found after multiplying correlation tables together is the same as the peak correlation value in one of the combined tables is remote. Furthermore, valid vectors are removed only when tracer particle displacement is obscured in all of the combined correlation tables. Consequently, this method of spurious vector detection is highly effective and results in little data loss.

When the data from the previous example is processed using peak comparison, 100% of the spurious vectors are removed and less than 2% of the valid vectors are removed. The result is a 6% increase in the number of valid vectors calculated using correlation error correction even after 100% of the spurious vectors are removed.

Spatial Resolution

As a way of illustrating the improvement in spatial resolution resulting from correlation error correction through velocity gradient enhancement, consider the two interrogation regions that overlap by 25% shown in Fig. 7. A velocity field can be artificially imposed such that particle displacement is one particle image diameter in the negative direction in the left region, $Dv_L=-d$, and one particle image diameter in the positive direction in the right region, $Dv_R=+d$. As illustrated in Fig. 8, calculated particle displacement of the left and right regions when processed without correlation error correction is almost unaffected by any velocity imposed on the overlapping region (Dv_o). When processed with correlation error correction, however, the resulting calculated displacement closely matches the imposed velocity in the overlapped region and does not equal the average of the imposed displacements on the left and right regions. Since the overlapped region is only

25% of the area of either the left or right regions, spatial resolution is effectively improved by 75%.

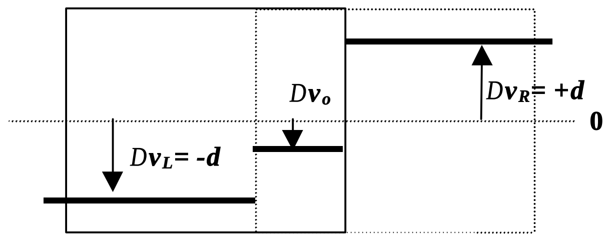

Figure 7. *– Schematic of imposed velocity on two interrogation regions that overlap 25%. This imposed velocity profile is used to illustrate the enhanced spatial resolution resulting from correlation error correction (Fig. 8).*

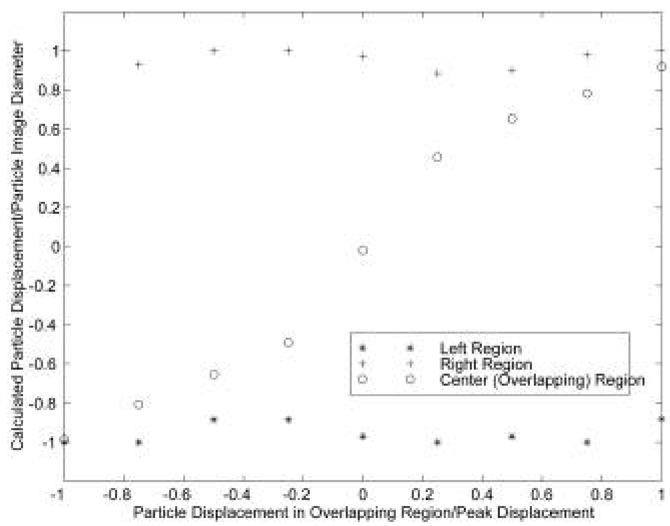

Figure 8. *– Illustration of improved effective spatial resolution by velocity gradient enhancement. The calculated particle displacement using correlation error correction (shown as 'o') follows the imposed velocity in the overlapped region in Fig. 7 and is not an average of the velocities imposed on the left and right regions (shown as '*' and '+' respectively).*

Out-of-Boundary Particle Motion

Fig. 9 illustrates the effect of translation on subpixel accuracy by comparing uncorrected results with results corrected from fifty-percent overlapping regions.

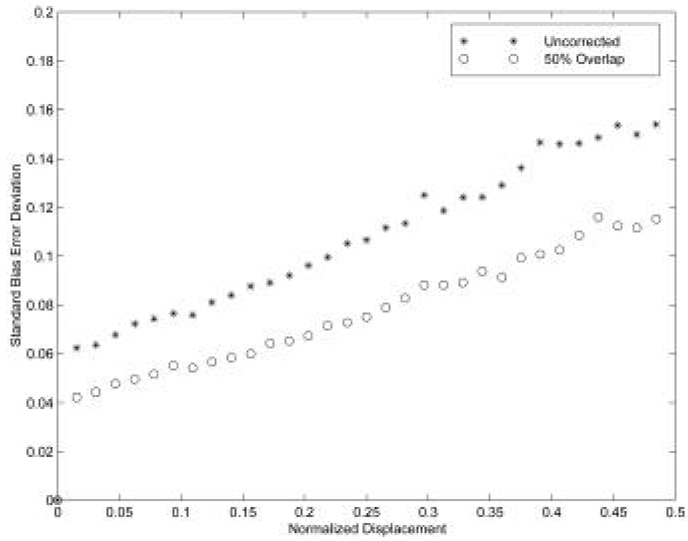

***Figure 9**. – Effect of translational displacement on subpixel accuracy. Correlation error correction improves subpixel accuracy by eliminating anomalies in the correlation table and strengthening the peak correlation signal.*

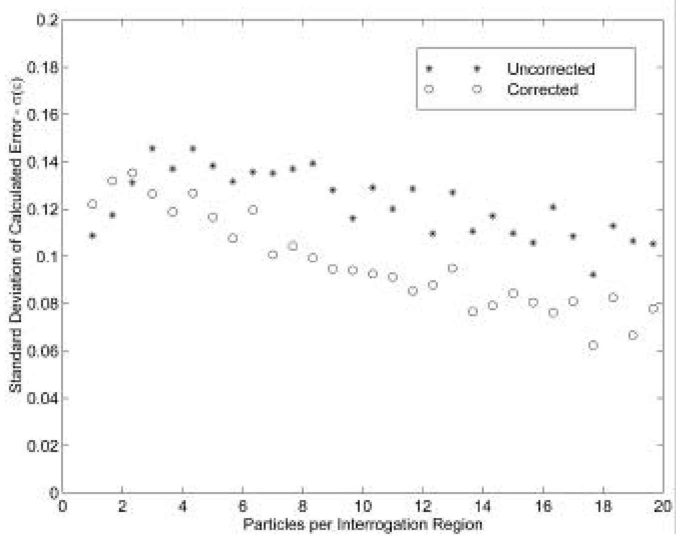

***Figure 10.** – Effect of seeding density on subpixel accuracy.*

Here the standard deviation of the displacement error from one thousand interrogation regions are plotted as a function of imposed particle translational displacement normalized by the interrogation size (64 *px*). The correlation error corrected results show a twenty-five percent improvement in resolving subpixel displacement. Note that the bias error increases linearly with translational displacement. This is consistent with errors conjectured by Adrian (1991) and analyzed in detail by Westerweel, Dabiri, and Gharib (1997). It is, to some extent, the result of fewer matching particle image pairs between correlated regions. In translational flow, particles are convected out of and into the interrogation region. These convected particles do not appear in both exposures and thus, not all of the particle images in a region contribute to the peak correlation value. Consequently, translational flow has a similar effect to a reduction in seeding density, Fig. 10.

Errors associated with translational motion exist for out-of-plane particle displacement as well. Out-of-plane motion is particularly limiting to PIV as it restricts measurements to regions of nearly planer flow and restricts the minimum width of the sample volume, thereby restricting spatial resolution.

As shown in Fig. 11, correlation error correction is highly effective at resolving particle displacements from regions with significant out-of-plane flow. Here the percentage of valid vectors is plotted as a function of normalized out-of-plane translational particle displacement. The uncorrected data begins to produce excessive spurious results at fifty-percent displacement. Using fifty-percent overlapped regions, correlation error corrected data produces few spurious results until almost 90% displacement. At 100% displacement, flow information is lost as all of the particles within the interrogation region are transported out between exposures.

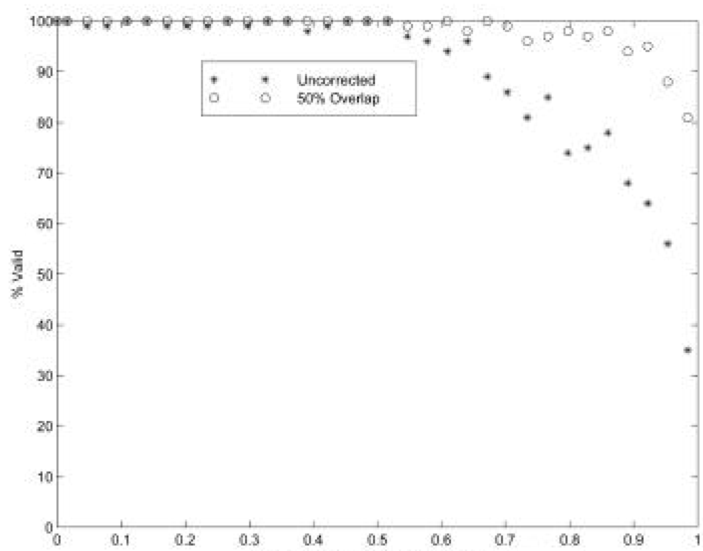

Figure 11. *– Effect of out-of-plane flow on PIV processing. Correlation error correction using fifty-percent overlapped regions significantly improve the ability to resolve particle displacements.*

Velocity Gradient Effects

While highly effective at resolving displacements from regions with significant out-of-plane motion, for a fixed interrogation size, correlation error correction is somewhat less effective at resolving regions of high velocity gradients. Fig. 12 shows a plot of the percentage of valid vectors as a function of normalized velocity gradient in the ***ij*** interrogation plane;

$G_\nabla = \dfrac{m\left|\nabla \bar{v}_{ij}\right| N\Delta t}{d}$ where *N* is the interrogation size (64 *px* in this case), *m* is the image magnification, *Dt* is the time between exposures, and *d* is the average imaged particle diameter. As shown, correlation error correction increases the number of valid vectors calculated from regions of high velocity gradients. Above a gradient level of about $G_{\tilde{N}}=1.2$, however, the probability of acquiring a valid vector quickly diminishes. A distinct advantage of correlation error correction, however, is that the improvement of the correlation signal strength allows smaller interrogation regions to be used. These smaller regions can resolve higher velocity gradients. Consequently, the simple analysis presented here does not accurately reflect the improvement in resolving velocity gradients that results from the use of correlation error correction. Such improvement depends largely on the seeding density of the flow.

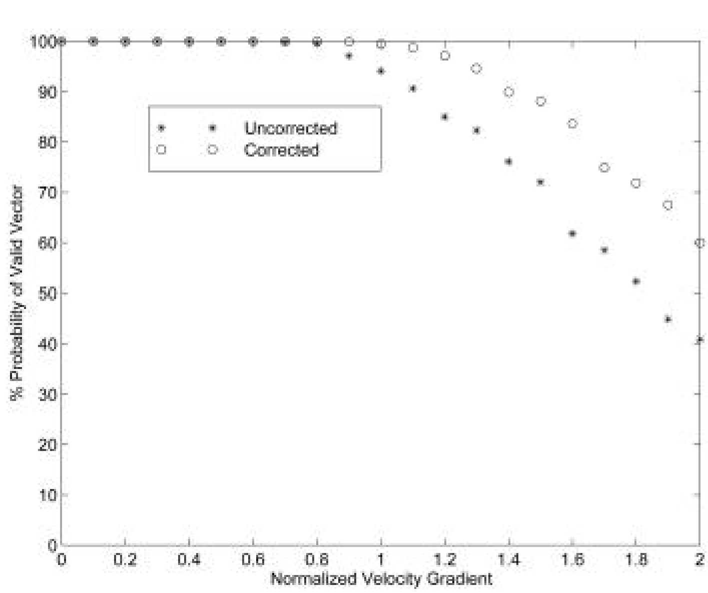

Figure 12. – *Effect of velocity gradient on PIV processing. Correlation error correction improves the ability to resolve tracer particle displacements in regions that have high velocity gradients.*

5 Experimental Demonstration: *High Accuracy/ High Resolution Processing*

The robustness of correlation error correction in removing spurious vectors and correlation anomalies allows the use of recursive correlation processing to iteratively arrive at local particle displacement without generating spurious results; a region is correlated, the interrogation window size is then reduced and offset by the previous result before re-correlating with the new window over a reduced region. Each correlation depends on the accuracy of the proceeding result. Without a highly robust and efficient means of detection, errors quickly propagate. With the aid of correlation error correction, the result of this correlation process can be quite dramatic as is illustrated in Fig. 13. Here recursive correlation along with correlation error correction is used to iteratively resolve the velocity of a swirling flow undergoing sudden expansion (backward step at bottom of figure).

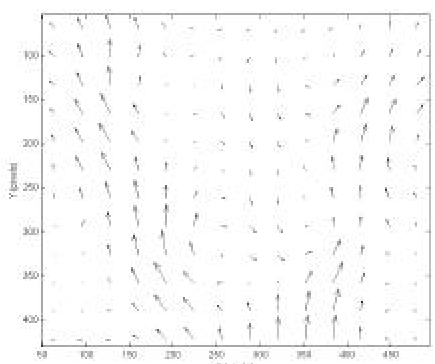

(A) ***150 vectors (64x64 pixel sub-windows)***

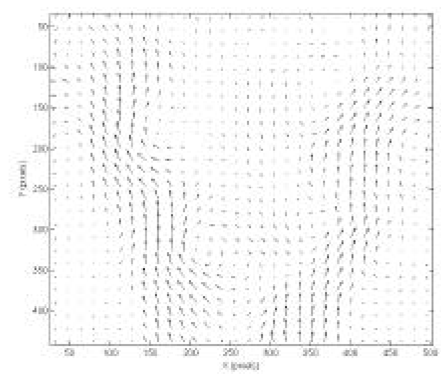

(B) ***750 vectors (32x32 pixel sub-windows)***

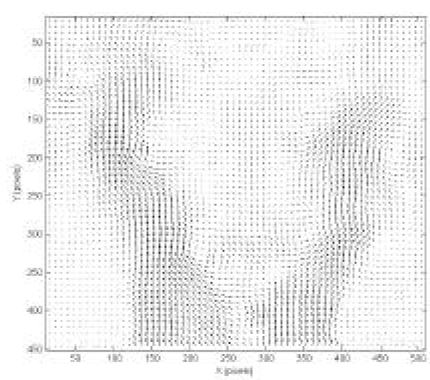

(C) ***3,350 vectors (16x16 pixel sub-windows)***

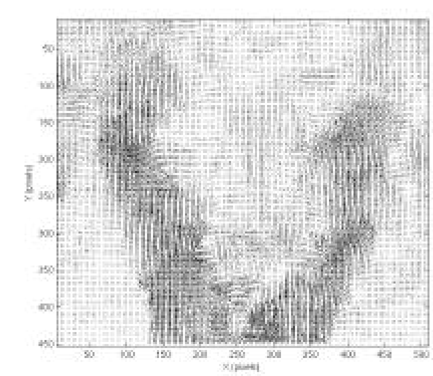

(D) ***15,000 vectors (8x8 pixel sub-windows)***

Figure 13. *– Recursive processing (A to D) of a PIV image of a swirling flow undergoing sudden expansion (Re=35,000, W=2.4).*

Figure 14 shows the same data resolved almost to the level of single particles (4*x*4 *pixel)*. 60,000 vectors are displayed each representing a 0.8mm^3 region of the flow. Using sparse array image correlation, results from the entire image are processed in less than one minute (>1,000 vectors/sec) [Hart, 1996]. Although it is unlikely that the images used to process this data contain information to the resolution implied by this plot, it illustrate the possibility of processing PIV to the limits of optical resolution without generating excessive errors even, as in this case, when significant out of plane flow exists.

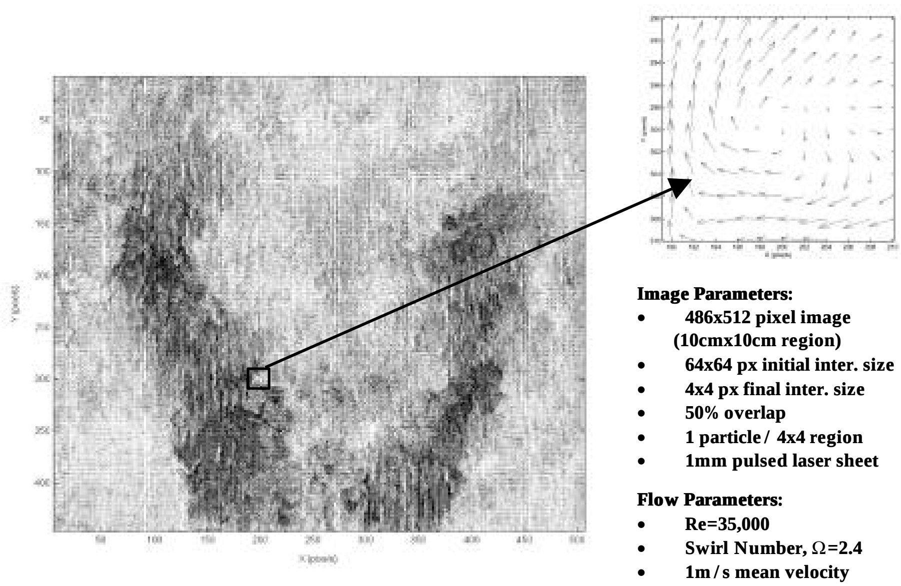

Figure 14. *– 60,000 vectors calculated from a 486x512 image of a swirling flow (Re=35,000, W=2.4) undergoing sudden expansion using recursive correlation. Each vector on average represents a single tracer particle in the flow and is the result of as many as five sub-window correlations. These results are processed at a rate of over 1,000 vectors/sec using sparse array image correlation with correlation error correction.*

6 Conclusions

Stochastic correlation values can be eliminated during PIV processing by element-by-element multiplication of correlation tables calculated from adjacent regions. This correction method, which is essentially a correlation of two or more adjacent correlation tables, improves subpixel accuracy and eliminates spurious vectors resulting from unmatched particle pairs, out-of-boundary motion, particle overlap, inter-particle correlations, and electronic and optical imaging noise. Particle displacement information that does not correlate equally in the combined regions is minimized. The resulting calculated displacement is weighted to the adjoining area improving the effective spatial resolution in regions of high velocity gradients.

Correlation error correction, unlike post-interrogation methods, uses all available correlation information calculated from interrogation regions and does not rely on the accuracy or similarity of neighboring vectors. Consequently, it resolves tracer particle displacement from regions that are otherwise obscured by correlation anomalies. Thus, the correction method presented herein reduces bias errors and eliminates spurious vectors while improving spatial resolution and vector yields.

References

Adrian, R. J. (1991) "Particle imaging techniques for experimental fluid mechanics," *Annual Review of Fluid Mechanics* Vol. 23, pp. 261-304.

Fincham, A. M.; Spedding, G. R. (1997) "Low Cost, High Resolution DPIV for Measurement of Turbulent Flow," *Experiments in Fluids*., Vol. 23, pp. 449-462.

Fincham, A. M.; Spedding, G. R.; Blackwelder, R. F. (1991) "Current Constraints of Digital Particle Tracking Techniques in Fluid Flows," *Bull Am Phys Soc.* Vol. 36, 2692.

Hart, D.P., (1996) "Sparse Array Image Correlation," 8th International Symposium on Applications of Laser Techniques to Fluid Mechanics, Lisbon, Portugal.

Keane, R. D.; Adrian, R. J., (1990) "Optimization of Particle Image Velocimeters," *Measurement Science and Technology*, Vol. 2, pp. 1202-1215.

Keane R.D.; Adrian, R.J., (1992) "Theory of cross-correlation of PIV images," *Applied Scientific Research*, Vol. 49, pp. 191-215.

Landreth, C. C.; Adrian, R. J., (1990) "Measurement and Refinement of Velocity Data Using High Image Density Analysis in Particle Image Velocimetry," Applications of Laser Anemometry to Fluid Mechanics, Springer-Verlag, Berlin, pp. 484-497.

Okamoto, K; Hassan, Y. A.; and Schmidl, W. D., (1995) "New Tracking Algorithm for Particle Image Velocimetry," *Experiments in Fluids*., Vol. 19, pp. 342-347.

Prasad, A.K.; Adrian, R.J.; Landreth, C.C.; Offutt, P.W., (1992) "Effect of Resolution on the Speed and Accuracy of Particle Image Velocimetry Interrogation," *Experiments in Fluids*, Vol. 13, pp. 105-116.

Raffel, M.; Kompenhans, J., (1994) "Error Analysis for PIV recording Utilizing Image Shifting," Proc. 7th International Symposium on Applications of Laser Techniques to Fluid Mechanics, Lisbon, July, p. 35.5.

Westerweel, J. (1994) "Efficient Detection of Spurious Vectors in Particle Image Velocimetry Data," *Experiments in Fluids*., Vol. 16, pp. 236-247.

Westerweel, J.; Dabiri, D.; Gharib, M., (1997) "The Effect of a Discrete Window Offset on the Accuracy of Cross-Correlation Analysis of Digital PIV Recordings," *Experiments in Fluids*, Vol. 23, pp. 20-28.

Willert, C. E.; Gharib, M. (1991) "Digital Particle Image Velocimetry," *Experiments in Fluids*, Vol. 10, pp. 181-193.